Supporting Information for

Pentachlorophenol radical cations generated on Fe(III)-montmorillonite initiate octachlorodibenzo-*p*-dioxin formation in clays: density functional theory and Fourier transform infrared studies

Cheng Gu,[†] Cun Liu,[†] Cliff T. Johnston,[,‡] Brian J. Teppen,[*,†] Hui Li,[†] and Stephen A. Boyd[*,†]*

†Department of Crop and Soil Sciences, Michigan State University, East Lansing, MI 48824

‡Crop, Soil and Environmental Sciences, Purdue University, 915 W. State Street, West Lafayette, IN 47907

[*]To whom correspondence should be addressed.

Cliff T. Johnston
Phone: (765) 496-1716
Fax: (765) 496-2926
E-mail: clays@purdue.edu

Brian J. Teppen
Phone: (517) 355-0271 ext. 254
Fax: (517) 355-0270
E-mail: teppen@msu.edu

Stephen A. Boyd
Phone: (517) 881-0579
Fax: (517) 355-0270
E-mail: boyds@msu.edu

Summary

Supplemental Information for Materials and Methods S-3

Supplemental Information for Results and Discussion S-5

Figure SI 1. Atom numbering scheme for pentachlorophenol (PCP) S-7

Figure SI 2. Integrated intensities of selected IR bands in homoionic Fe(III)-montmorillonite clay/pentachlorophenol S-8

Figure SI 3. Optimized geometries of pentachlorophenol (PCP), PCP/H_2O and PCP/$Fe(OH)(H_2O)_n^{2+}$ in the gas phase S-9

Figure SI 4. Potential energy profiles for stable conformers of PCP/$FeOH^{2+}$ complexes. S-10

Table SI 5. Additional geometry parameters of PCP/$Fe(OH)(H_2O)_n^{2+}$ in gas phase (for structures refer to SI 3). S-11

Figure SI 6. Molecular orbital energy level diagrams (the d block) for bare $FeOH^{2+}$ (left) and PCP/$FeOH^{2+}$ (right) systems. S-12

Figure SI 7. DFT calculated infrared spectra of selected PCP/$Fe(OH)(H_2O)_n^{2+}$ systems with the number of coordination water n equal to 3(a), 2(b), 1(c) and 0(d) (for structures refer to SI 3). S-13

Figure SI 8. Optimized structures of ONIOM models of the pentachlorophenol/radicals adsorbed on clay surface S-14

Table SI 9. Selected computed geometry parameters of ONIOM pentachlorophenol (PCP)-smectite clay clusters S-15

References to Supplemental Information S-16

Supplemental Information for Materials and Methods

Preparation of Self-supporting Clay films. Smectite clay (Wyoming montmorillonite, SWy-2) was obtained from the Source Clays Repository of the Clay Minerals Society (Purdue University, West Lafayette, IN). The preparation of Fe(III)-montmorillonite followed the method of Arroyo *et al.* (*1*) Briefly, the clay suspension was first titrated to pH 6.8 with 0.5 M sodium acetate buffer (pH 5) to remove carbonate impurities. Clay-sized particles (<2 μm) were obtained by centrifugation for 6 min at 60 g, then treated with 0.1 M $FeCl_3$ solution six times. The Fe(III)-saturated Swy-2 was washed using Milli-Q water until free of chloride as indicated by a negative test with $AgNO_3$, then freeze-dried.

Self-supporting clay films were prepared by the procedures developed previously (*2, 3*). Twenty ml of clay-PCP aqueous suspension containing 35 mg of the Fe(III)-Swy-2 clay and 0.35 mmol L^{-1} of PCP (Aldrich, Milwaukee, WI, purity >98%) were passed through a 0.45 μm hydrophilic polyethersulfone membrane filters (47 mm in diameter). To maximize the PCP loading, the filtered solution was passed through the membrane three more times. The resulting clay-PCP deposit on the filter was allowed to air-dry overnight and then removed from the filter by running the filter and clay deposit over a knife edge (*4*).

Computational methods on interactions between PCP/PCP radicals and clay surface. In a study that is independent of the spectroscopic calculations using PCP/$Fe(OH)(H_2O)_n^{2+}$ clusters in the main part of this paper, adsorption of PCP radicals to a clay surface fragment was modeled in order to estimate the relative stabilization of each radical intermediate by the clay surface. A neutral aluminosilicate fragment was used as a model for the clay because only weak electrostatic interactions between PCP and clay siloxane surfaces have been observed (*5*). In the two-layered ONIOM model, a neutral smectite cluster model interacting with PCPs was constructed as the real system and the adsorbate PCP species were taken as the model system. The Hartree-Fock method and basis sets of 3-21G and 6-31G were applied to the outer and inner layers, respectively. The clay structure was derived from full relaxation of a periodic model for the neutral clay mineral pyrophyllite. The cluster consisted of 6.5 half unit cells with a formula $6.5(Al)_2(Si)_4O_{10}(OH)_2 \cdot nH_2O$, containing exactly three ditrigonal hexasiloxane rings on each tetrahedral sheet.

Supplemental Information for Results and Discussion

ONIOM calculations on PCP/PCP radicals interacting with clay surface. To explore the apparent role of clay surfaces in stabilizing radical cation intermediates, we compared PCP, its radical cation, and the phenoxy radical on a clay mineral surface as modeled by the ONIOM method. Resulting configurations and structure parameters of PCP are shown in supporting information SI 8 and 9. The calculated bond lengths of a single PCP molecule adsorbed on clay mineral surface were uniformly ~0.2 Å shorter than those of isolated PCP, which results from overestimation of bond strength by the Hartree-Fock method used in the ONIOM model. The average C-C bonds in the PCP radical cation on the clay mineral surface were elongated by 0.026 Å compared with those of neutral PCP on the clay, due to the loss of one π electron (as observed in the absence of clay, Table 1). Both PCP and the PCP radical cation formed hydrogen bonds with the surface oxygen with the H_1-$O_{surface}$ bond length equal to 1.724 Å and 1.535 Å, respectively (supporting information SI 9), and the benzene plane of each molecule tilted about 30-31 degrees toward the clay mineral surface due to the hydrogen bond. The PCP phenoxy radical adopted a conformation parallel to the clay mineral surface with a distance of 3.06 Å (from O_1 to the surface oxygen plane) which is longer than those of 2.67 Å and 2.69 Å for PCP and the PCP radical cation (supporting information SI 9), suggesting a weaker adsorption of the PCP phenoxy radical. The calculated adsorption energies were -14.6 kcal/mol, -56.4 kcal/mol and -6.9 kcal/mol for PCP, PCP radical cation and PCP phenoxy radical, respectively (supporting information SI 9), and compared to the isolated PCP in gas phase the ionization energy of PCP on clay was decreased by 39.2 kcal/mol showing a much stronger stabilization of the PCP radical cation compared to the other species, due to more favorable electrostatic interactions with the (negatively charged) clay mineral surface. The relatively weak interaction between the neutral PCP molecule and the clay mineral surface supports our usage of Fe(III)/PCP complexes alone (not explicitly accounting for the effects of clay mineral surfaces) to predict the spectroscopic properties of the complicated PCP interactions with interlayer iron in smectite. That is, the role of clay may not be to influence any local structural interactions between Fe and PCP, but we hypothesize that the electrostatic field in the clay interlayer may strongly direct the reactivity along the radical cation pathway rather than the phenoxy radical pathway that might otherwise be favored in the absence of clay.

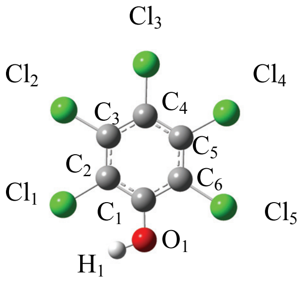

SI 1. Atom numbering scheme for pentachlorophenol (PCP).

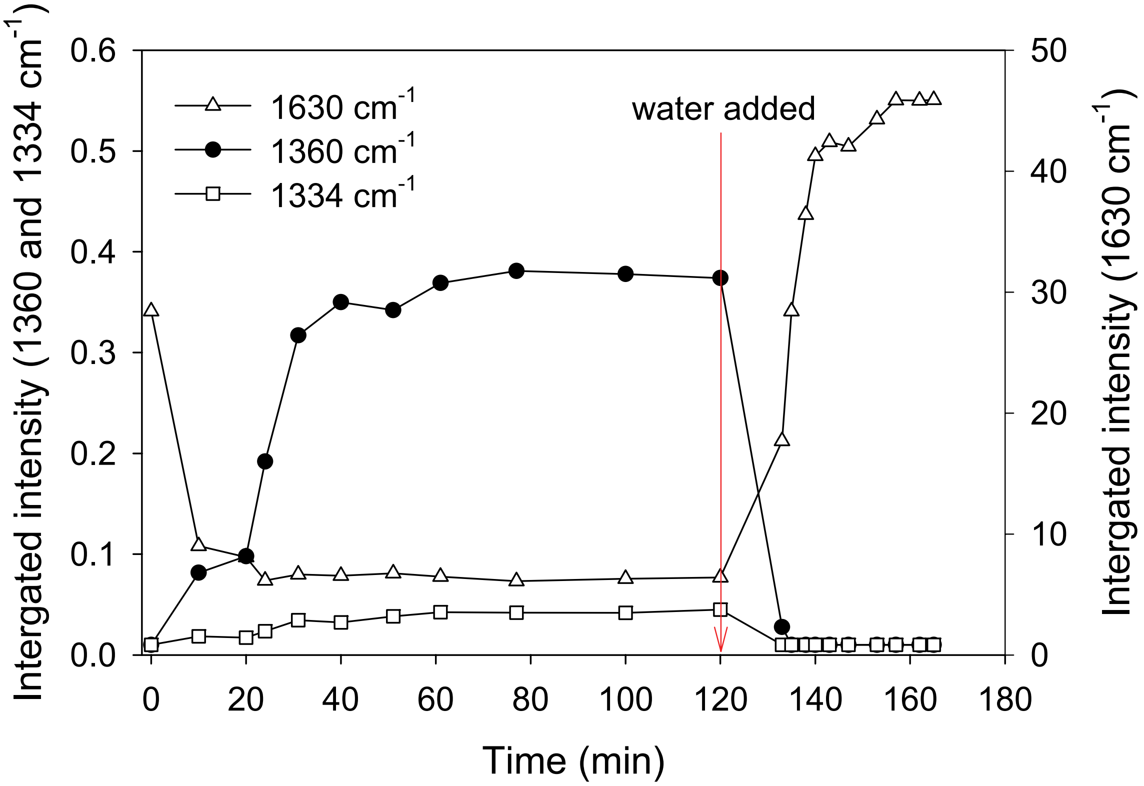

SI 2. Integrated intensities of selected IR bands in homoionic Fe(III)-montmorillonite clay/pentachlorophenol as a function of exposure time to vacuum ($0 < t < 120$ min) and water vapor ($t > 120$ min).

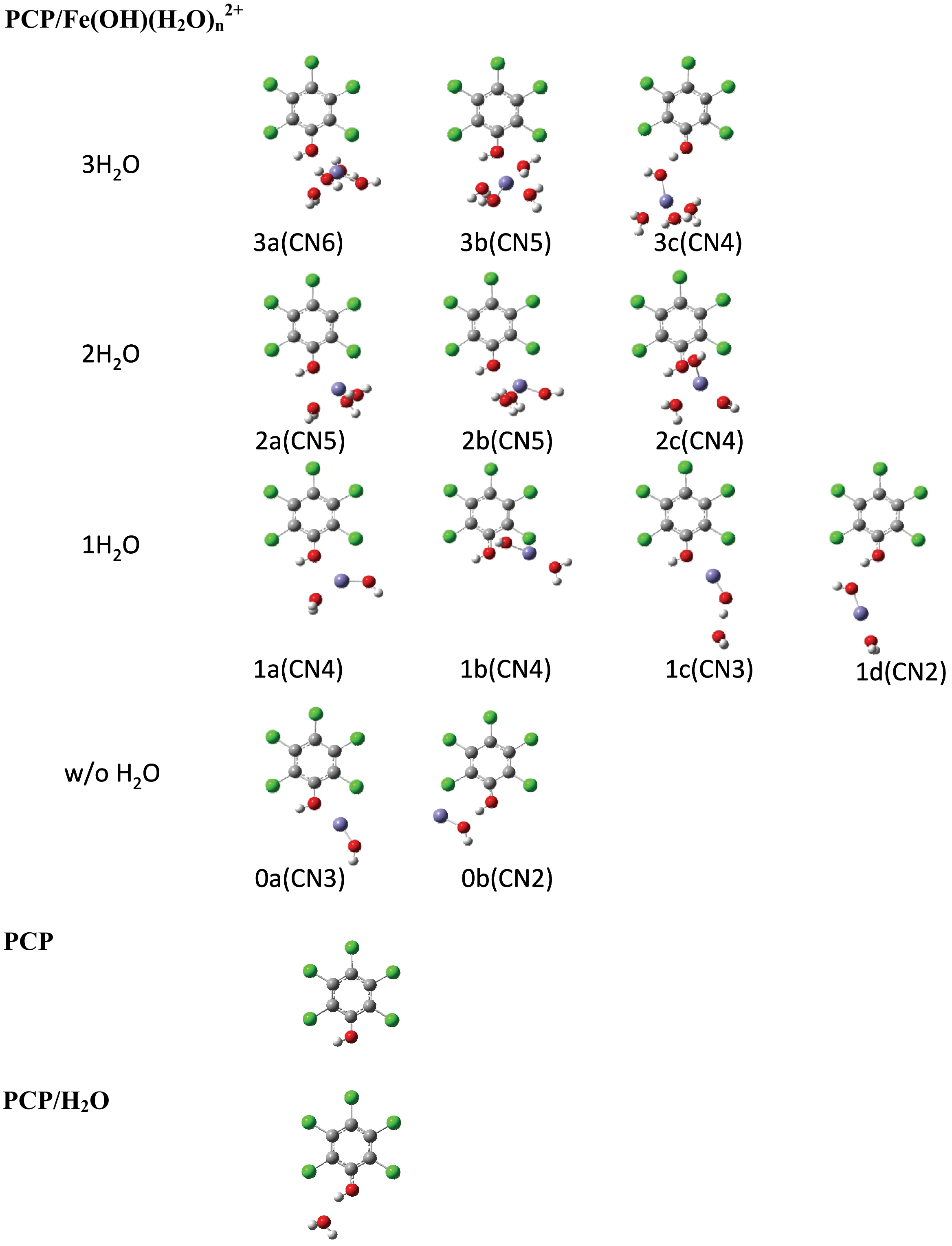

SI 3. Optimized geometries of pentachlorophenol (PCP), PCP/H_2O and PCP/Fe(OH)$(H_2O)_n^{2+}$ in the gas phase. Color scheme is: dark gray=carbon; green=chlorine; red=oxygen; light gray=hydrogen.

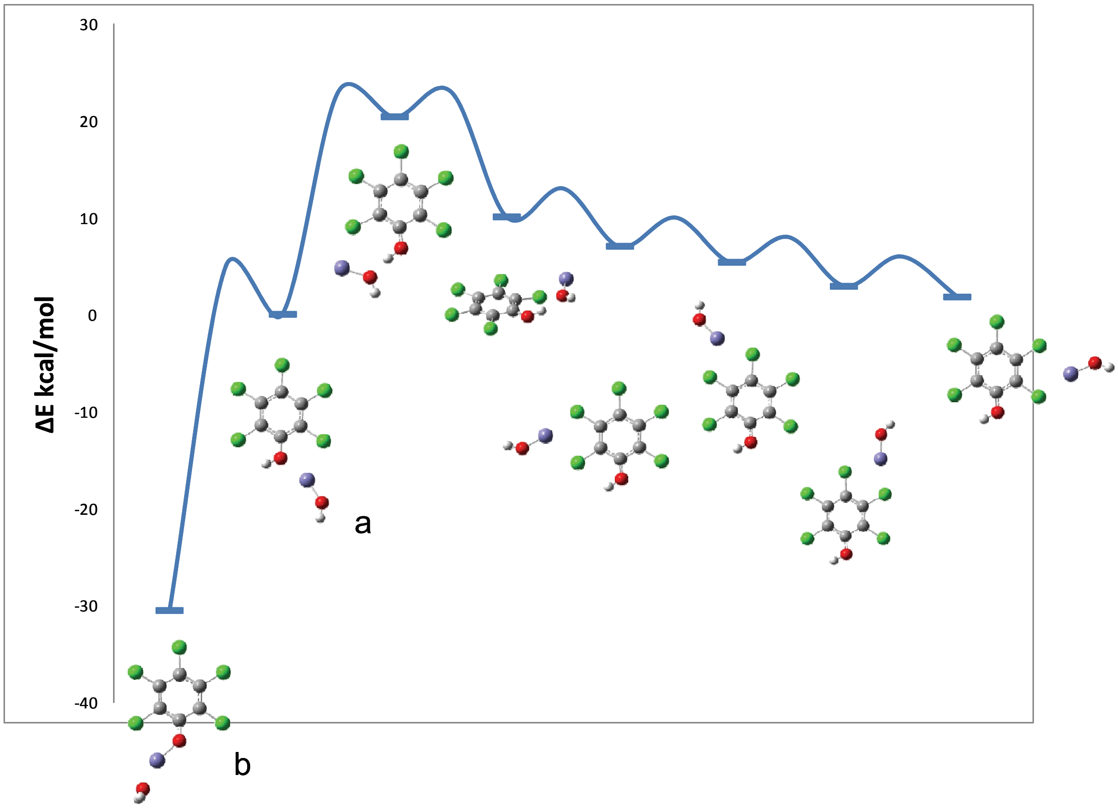

SI 4. Potential energy profile for the stable conformers of PCP/FeOH^{2+} complexes. The configuration a is the collinear structure of the pentachlorophenol (PCP) cation radical with FeOH^{+}, and the configuration b is the PCP phenoxy radical with FeOH$_2^{2+}$.

SI 5. Additional geometry parameters of PCP/Fe(OH)$(H_2O)_n^{2+}$ in gas phase (for structures refer to SI 3). (unit: distances (Å), angles (degree) and energies (kcal/mol))

Complex ID	CN	Spin on pcp	spin on Fe	Relative energy*	Angle O-Fe-O	Distance Fe-O
3a	6	0.46	3.84		162.11	2.18
3b	5	0.6	3.83	5.17	135.64	2.31
3c	4	1	3.72	-21	32.30	3.88
2a	5	0.74	3.73		138.03	2.21
2b	5	0.6	3.80	2.78	160.51	2.22
2c	4	0.99	3.68	-1.62	84.98	2.48
1a	4	1.04	3.61		138.54	2.40
1b	4	1.03	3.66	-5.15	61.42	3.88
1c	3	0.92	3.60	20.51	156.89	2.15
1d	2	1	3.72	-9.66	36.64	4.04
0a	3	1.04	3.58		162.62	2.18
0b	2	1.07	3.69	21.06	36.25	3.79

* Relative energy was calculated by assigning the total energy of the optimized "a" structure as zero.

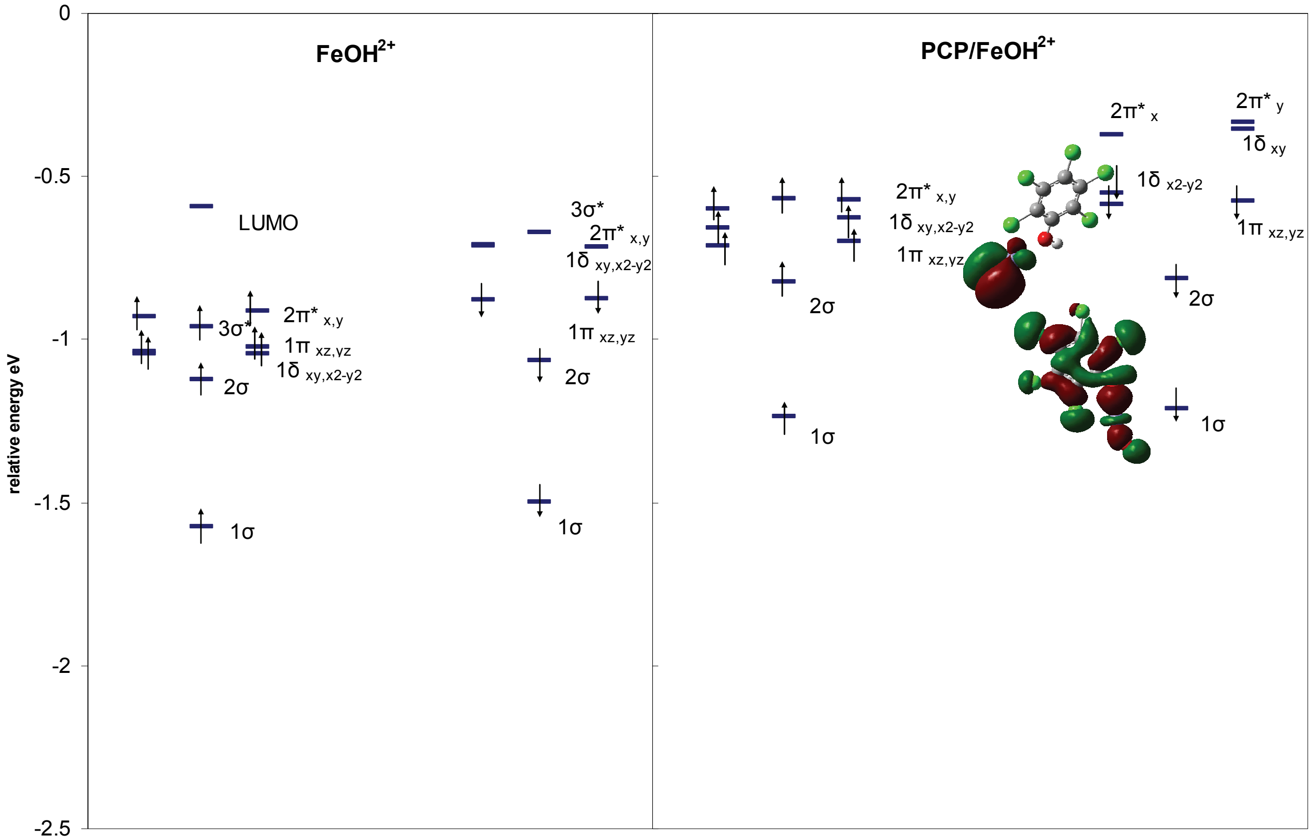

SI 6. Molecular orbital energy level diagrams (the d block) for bare $FeOH^{2+}$ (left) and $PCP/FeOH^{2+}$ (right) systems. The insets on the right panel show the 1δ and 2σ molecular orbitals. One electron transferred from PCP molecule fills into the non-bonding 1δ orbital, which is localized primarily on the Fe $d_{x^2-y^2}$ orbital. The 2σ molecular orbital consists of collinear overlaps between Fe d_{z^2} and PCP oxygen p_z orbitals.

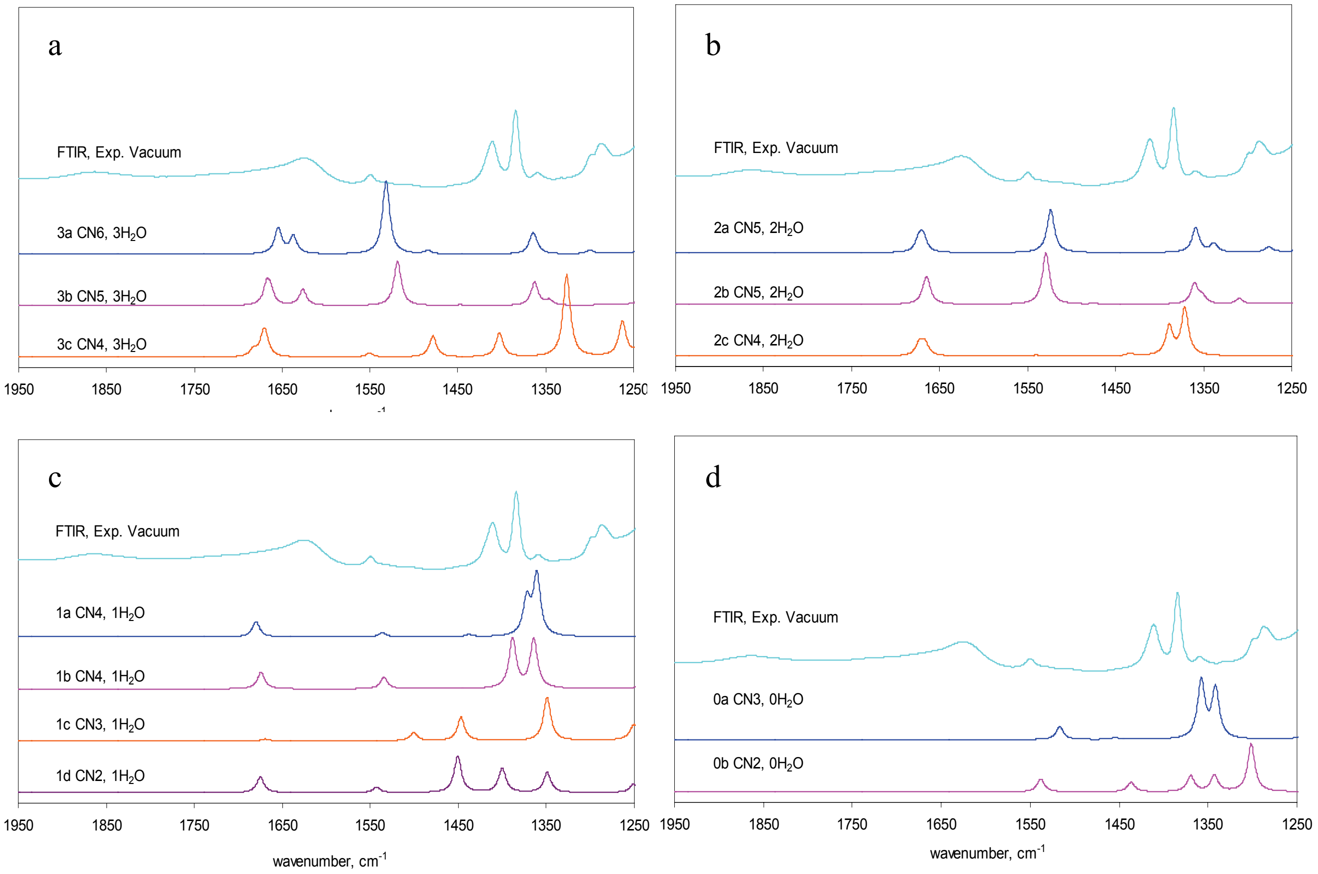

SI 7. DFT calculated infrared spectra of selected PCP/Fe(OH)(H_2O)$_n^{2+}$ systems with the number of coordination water n equal to 3(a), 2(b), 1(c) and 0(d) (for structures refer to SI 3).

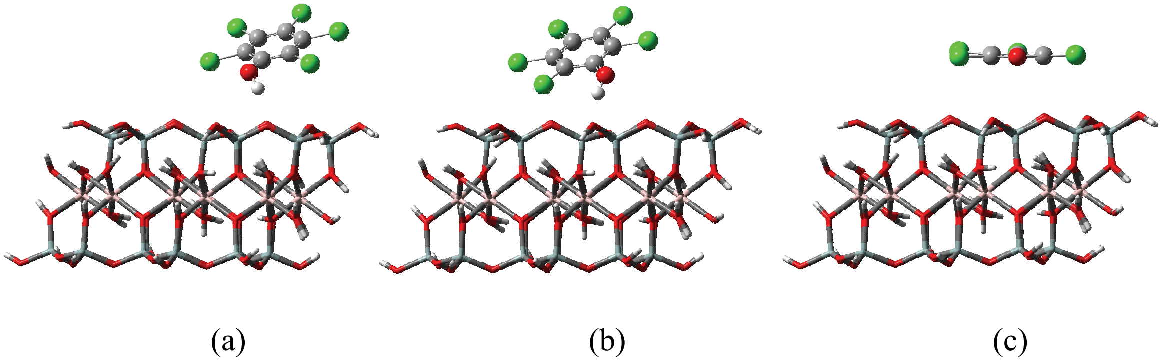

SI 8 ONIOM models of the pentachlorophenol (PCP) molecule (a) PCP radical cation (b) and PCP phenoxy radical adsorbed on smectite clay surface. Color scheme for PCP: red=O; green=Cl; dark gray=C; light gray=H. The 2:1 aluminosilicate clay layer is shown below the PCP structures. Color scheme for the clay layer: red=O; dark gray=Si; light gray=H; pink=Al.

SI 9. Selected computed geometry parameters of ONIOM pentachlorophenol (PCP)-smectite clay clusters (units: distances (Å) and angles (degree) energies (kcal/mol)).

Parameter	**ONIOM PCP-smectite cluster**		
	PCP	PCP cation radical	PCP phenoxy radical
bond length			
C_1-O_1	1.345	1.270	1.292
O_1-H_1	0.966	1.014	
C_1-C_2	1.387	1.437	1.428
C_2-C_3	1.381	1.373	1.390
C_3-C_4	1.382	1.419	1.409
C_4-C_5	1.387	1.417	1.409
C_5-C_6	1.379	1.376	1.391
C_6-C_1	1.390	1.440	1.429
distance of PCP-H$\cdots$$O_{surface}$	1.724	1.548	
angle between PCP ring and surface oxygen plane	29.91	31.41	2.71
distance between PCP-O and surface oxygen plane	2.67	2.29	3.06
adsorption energy	-14.6	-56.4	-6.9

References to Supplemental Information

(1) Arroyo, L. J.; Li, H.; Teppen, B. J.; Boyd, S. A. A simple method for partial purification of reference clays. *Clays Clay Miner.* **2005**, *53*, 511-519.

(2) Johnston, C. T.; Tipton, T.; Trabue, S. L.; Erickson, C.; Stone, D. A. Vapor-phase sorption of p-xylene on Co- and Cu-exchanged SAz-1 montmorillonite. *Environ. Sci. Technol.* **1992**, *26*, 382-390.

(3) Fernandes de Oliveira, M.; Johnston, C. T.; Premachandra, G. S.; Teppen, B. J.; Li, H.; Laird, D. A.; Zhu, D.; Boyd S. A. Spectroscopic study of carbaryl sorption on smectite from aqueous suspension. *Environ. Sci. Technol.* **2005**, *39*, 9123-9129.

(4) Johnston, C. T.; Aochi, Y. O. Fourier transform infrared and Raman spectroscopy. In *Methods of Soil Analysis Part 3 Chemical Methods;* Sparks, D. L., Ed.; Soil Science Society of America: Madison, WI, 1996; pp 269-321.

(5) Zielke, R. C.; Pinnavaia, T. J. Modified clays for the adsorption of environmental toxicants: binding of chlorophenols to pillared delaminated, and hydroxyl-interlayered smectites. *Clays Clay Miner.* **1988**, *36*, 403-408.